ISSN: 2641-1784

Research Article

Advance in Environmental Waste Management & Recycling

Effect of the Processing Parameters of Doping Lime, Calcium and Zinc of Aluminium Alloys Recovered from Scrap

Mahmoud A. Rabah*

Chemical and Electrochemical Lab, Mineral Processing Dept. Centra; Metallurgical Research and Development Institute (CMRDI), Cairo, Egypt.

***Corresponding author**
Mahmoud A. Rabah, Chemical and Electrochemical Lab, Mineral Processing Dept. Centra; Metallurgical Research and Development Institute (CMRDI), P.O. Box 78 Helwan, Cairo, Egypt. Phone +201097704500.

Submitted: 18 Nov 2022; **Accepted**: 30 Nov 2022: **Published**: 12 Dec 2022

Citation: Rabah, M.A. (2022). Effect of the Processing Parameters of Doping Lime, Calcium and Zinc of Aluminium Alloys Recovered from Scrap. *Adn Envi Was Mana Rec*, 5(3), 352-366.

Abstract

The present work shows the effect of the processing parameters of separately doping lime, calcium and zinc on the properties of an aluminium alloy recovered from scrap. Two routes viz pyrometallurgy and powder metallurgy were involved the parameters displayed by the concentration of the alloying agents, time and temperature have been studied. Results showed that powder metallurgy promotes a wide spectrum for doping the host alloy. The doping process of lime to the molten aluminium needs more time as compared to the zinc metal. A heterogeneous structure of the eutectic phase developed with lime or calcium gradually affects the mechanical properties of the Al alloy. It decreased the density by 15.5 %, and increases its hardness to about 37 V. Calcium formed a eutectic phase Al4Ca at lower concentrations. The eutectic (Al)+Al4Ca of fine structure and the particles of Al4Ca are capable of spheroidization during heat treatment at ≥ 500 °C. The maximum hardness observed with lime-containing Al alloy gives a reason to expect a slight increase in mechanical strength properties. In the powder metallurgy method, Al was prepared by chemical victimization reducer hydrazine hydrate. The Al-Ca-Zn system is promising for the development of new eutectic type high-strength aluminium alloys. With zinc, the pyrometallurgy is far more convenient as compared to powder metallurgy. Zinc is uniformly distributed between aluminium solid solution and the intermetallic phases of the Al-Zn-Ca system. The activation energy of adding lime or calcium to the Al alloy amounts to 27.533, kJ/mol with a recovery potency of 98.7%. A process of annealing regenerated homogeneous structure when matched under a flux of carbon/alkali mix.

Keywords: Al 6061 Alloy from Scrap, Metal Turning Scrap, Alloys Recovery, the Effect of Calcium Addition. Properties of a recovered Alloy of Aluminium

Introduction

The Al alloy 6061 is the strongest aluminium alloy available (www. machine design 2007). . Yih and Wang Plenum Press, New York, 1979 reported that the hydrometallurgy and pyrometallurgy processes were successful methods to recover valuable metals from a scrap of tungsten carbide. The European Commission, EUR 24786 EN – 2011 showed that several member States proposed that there should be separate customs codes for scrap assortment. This could allow all enforcement personnel to figure with the identical parameters and reduce uncertainty scrap considered as wastage. This code would be in line with NACE codes 2011 and/or CN trade codes (CN Codes, 2011). Katiyara et al, ICNFMM-2014 claimed that the recovery of W and Co metals was paid out by either hydro or pyrometallurgical methods.

An electrochemical route has been established as a horny method because it should be one step dissolution process consuming very low energy. However, passivation is narrated to impede the dissolution rate and hence, some additives have also been tried for continuous dissolution. The zinc melt process method was disclosed by Edtmaier 2005 whereby molten zinc was rapidly alloyed with cobalt binder and embrittled the reinforced carbide. Both zinc and cobalt metals were removed by acid treatment, and only tungsten carbide could be reused directly. Barnard et al. 1971 Showed the recovery of zinc from Zn-Co alloy was carried out by the thermal distillation process. The hydrometallurgical route involved immersing the scrap I in a leaching solution to dissolve the matrix or binder material whereby the inactive residue of tungsten carbide formed. The metal carbide directly produced. Zinc substantially increases strength and permits precipitation hardness. The number of operations of the process was decreased. The chlorination method was also reported in US Patent, 3,560,199, 1971 by Jonsson 1971, where the scrap material was subjected to chlorination. The process took place at high temperatures in an exceeding chlorine

atmosphere to form metal chloride. (Leblanc 1971). The author reported the conceptual stages of the metal recycling process as follows; collection, sorting and shredding. The shredding step is completed to plug the melting process. Small shredded metals have a high surface to volume ratio, melting and purification. The influence of the temperature of the melt overheating and pouring on the quality of aluminium alloy castings was reported. The proper melting temperature was 880–890°C. Chen et al. 2019 showed that high billet temperature reduced the grain size and increased the volume fraction of Al23CuFe4 and Al-Mg-Zn alloys. Calcium addition up to 0.7 Wt. pct beneficiates applications of Ca as a modifier in Al-Si alloys. Iron neutralised the recycled aluminium alloys with high iron content, scavenger of Sb, P and Bi from secondary alloys. The interaction of Ca with other elements, the high-temperature oxidation, and the applications of Al–Ca alloys were discussed whereby other avenues for further work are recommended by Sreeja et.al. 2005. Because of its alkalinity, the addition of calcium shifted the fluid pH value of the alloy to a higher level. Electrochemical measurements revealed that increasing Ca content led to higher corrosion rates due to the formation of more cathodic Mg2Ca precipitate in the microstructure. The results suggested that Mg-0.7Ca with the minimum amount of Mg2Ca is a good candidate for bio-implant applications (Shervin et. al. 2013).

Laverty et. al 1989 claimed that the U.S. Bureau of Mines treated the mixed and contaminated superalloy scrap to separate and recover metal values. Results were obtained by leaching Zn or atomized scrap with HCl at 95O °C and 50 PSIG whereby approximately 98 % of the AI, Co, Cr, Cu, Fe, Mn, Ni, and Zn dissolved. while rejecting over 98 % of Mo, Nb, Ta, Ti, W, and Zr as an insoluble refractory residue. Chlorine successfully substituted HCI to leach Zn-treated scrap but was unsuccessful for leaching atomized scrap. The leaching solution was treated by pH adjustment to remove AI, Cr, Fe, and other contaminants as a filterable precipitate. Mashhad et. al 2009 recovered aluminium alloy scrap by applying cold pressing and proper melting salt flux. The authors showed that the major elements of the end products were AA336 aluminium alloy. Melting of cold-pressed specimens in salt flux produced samples with mechanical properties almost equal to the melting ingots. It had been claimed that research and survey of the quoted scrap, would impart huge data quoting prices of more than 250 types of ferrous, non-ferrous scrap and non-ferrous alloys. International metal scrap indexed DIN / ISO / EN / IS / ASME in both Metric & Imperial Inch sizes (Encyclopaedia, Internet online, 2021).

This work aims to study the effect of processing parameters on doping lime (calcium) and zinc on the physic-mechanical properties of Al 6061 alloy recovered from scrap. The activation energy of the investigated method has a special concern. A model of Al-Ca atoms arrangement in a face-cantered cubic (FCC) structure with a meting point of 585 °C and subsequent decrease in density has been elaborated. The properties of heating Al-alloy can further enhance the inclusion of a reinforcing phase that increases the mechanical properties of the alloys. The activation energy of the suggested method was also studied.

Experimental

The Al metal scrap composition.

The Al scrap material was obtained from the El-Maady Engineering company (military factory 54). About 30 kg of the scrap was collected. Table 1 shows the metal content of the metal scrap

Table 1: The Metal Content of The Scrap

Date of sample	Wt. %									.sample Wt., Kg
	Al	Si	Cu	Ni	Fe	Pb	Zn	Mg	Other	
March 2 2020	95.8-98.5	6.2	7.1	0.15	0.61	4.2	2.8	1.09	0.71	4
March 16 2020	96.05	0.8	--	0.62	0.24	1.06	0.8	0.15	0.01	5
April 16 2020	95.24	6.08	7.50	0.21	0.591	0.012	0.28	1.09	0.10	7
May 3 2020	98.55	7.75		0.72	0.20	0.59	0.10	0.267	1.0	7.5
May 18 2020	96.815	2.3		0.61	0.22	0.604	0.010	1.99	1.03	6.5
Collective Sample, (Kg)	19.47	5.99	1.90	0.21	0.60	0.01	0.24	1.05	0.73	30

Figure. (2a) Non-ferrous scrap

Figure.(2b) Ferrous and nonferrous metals

Figure 2: Photographs of the. Non-ferrous Scrap and Mixed Ferrous and Nonferrous Metals

Scrap Sorting

Commercially, scrap traders may sort metal scrap by various methods including magnets, or observe the metal's colour or weight to determine the metal type. For example, aluminium appeared silvery in lustre and light in weight, copper looks red whereas brass is yellow. The scrappers will be segregating clean metal from the dirty one to improve the value of their selling scrap. Sorting the ferrous metals from non-ferrous metals is an important step in that process.

Table 2. shows the innovative classification technique of consolidated and sorting methods. The physical parameter, the desired separation and the developed technology are reported for each method. Data elaborated from Haynes 2011.

Table 2: Classification of Consolidated and Innovative Sorting Methods

Method	Separator Type	Physical Parameter	Desired Separation
	air separator	mass	low density as paper, foam plastic
Consolidated methods	eddy current	conductivity	non-metal, and metal types

Dry grinding of the Al scrap

Usually, with dry grinding in the machine, the material will collide and hit other particles in a closed area until it has broken into the required size. Dry milling can thus make large-size particles reach micron size. But if smaller nano-meter sizes are targeted, the only way to achieve this goal is by wet grinding. Fig. 3 shows a Laboratory-scale fluidized bed jet mill

Figure. 3a The pilot-scale Grinding mill

Figure. 3b The ground scrap

Figure 3: The ALPA fine grinding MQW Fluidized Bed Jet Mill (Single Rotor / Multiple Roto ring mill).

The Chemicals

The chemicals used in this work were of pure grade, Table 3 shows the properties of the chem

Table 3: Properties of the Chemicals,

chemical	Source	Purpose	Property
Nitric acid H_2SO_4 HCl	SP.GR.1.18 (AR) Min. assay 36 % Fuming 69 % H_2SO_4 95-97% Extra pure SP.GR.1.18(AR) ADWIC	Leaching Process	ADWIC Riedel- de Hein ADWIC
Calcium metal Ca CO_3 EJSF2 Ca oxide	Green Egypt Sigma Aldrich	doping Synthesis process	ADWIC 99.3, 1.6 um 3.34 g/cm³, 1.57 um
NaOH Ammonium hydroxide	United Co. for chemicals & Med. Preparations		reagent for analysis 25 % Pure reagent for analysis
AgNO3 (Silver Nitrate)		Chloride ion determination	Pure reagent for analysis
distilled water		Chemical reactions	
Tap water		Other purposes	

Preparation of lime

Pure lime with a purity of 99.99% is synthesized by reacting pure calcium carbonate in pure HCl acid. The formed calcium chloride solution reacted with pure 30% ammonia to give calcium hydroxide gelatinous ppt. the solid ppt was washed with water many times, alcohol and dried to yield dry lime.

$$CaCl_2 + 2NH_4OH \longrightarrow Ca(OH)_2 + 2NH_4Cl \quad \ldots\ldots\ldots\ldots\ldots\ldots (1)$$

Preparation of the zinc metal

Chemically pure zinc element is prepared by thermal reduction of pure zinc oxide with active carbon according to

$$2ZnO + C^* \longrightarrow Zn + CO_2 \quad \ldots\ldots\ldots\ldots\ldots\ldots (2)$$

Method of the preparation of the Al-Ca-Zn alloys

The pyrometallurgy method (PM)

The collected Al scrap sample was washed with kerosene you get rid of grease contamination followed by washing with the sodium sulphonate detergent solution and rinsed with distilled water before drying under a nitrogen atmosphere. It was then milled to pass a mesh size of 40 microns and homogenized. The milled sample leached in ammonia /ammonium bicarbonate (1:1) altogether with 30% H_2O_2 to leach copper selectively. About 50 g of the clean and dry residue was placed in a SiC clean crucible of Salamander (1-litre capacity) and the scrap mass altogether with the lime, calcium or zinc was homogenized and covered with a solid flux powder made of ammonium chloride/ carbon (1:3) mix. The crucible with the metal charge is placed in a chamber furnace model Nabertherm LH fitted with a controller type C9, Germany maintained at the required temperature.

After the Al scrap melts, the molten contents are stirred with a porcelain spoonful. The crucible is returned to the hot chamber of the furnace for a more period. A sample of the molten Al alloy was periodically withdrawn for analysis. Similarly, the process was repeated with pure zinc. The Al alloys so formed were annealed at 550 °C- 600 °C for 10 h to improve the physical and mechanical properties of the doped aluminium

alloys, eliminate any inner stresses, reduce structural hardness, structural uniformity, ductility and fracture prevention (Wikipedia the free encyclopaedia, 2022). Structural uniformity improves ductility and fracture prevention (Axon et. al. 2022).

The powder metallurgy method (PoM)

Alternatively, the targeted alloy was made via powder technology. Fig. 4 shows a sequential processing diagram for the preparation of valuable 6061 alloys from metal scrap

The Properties of The Targeted Alloys

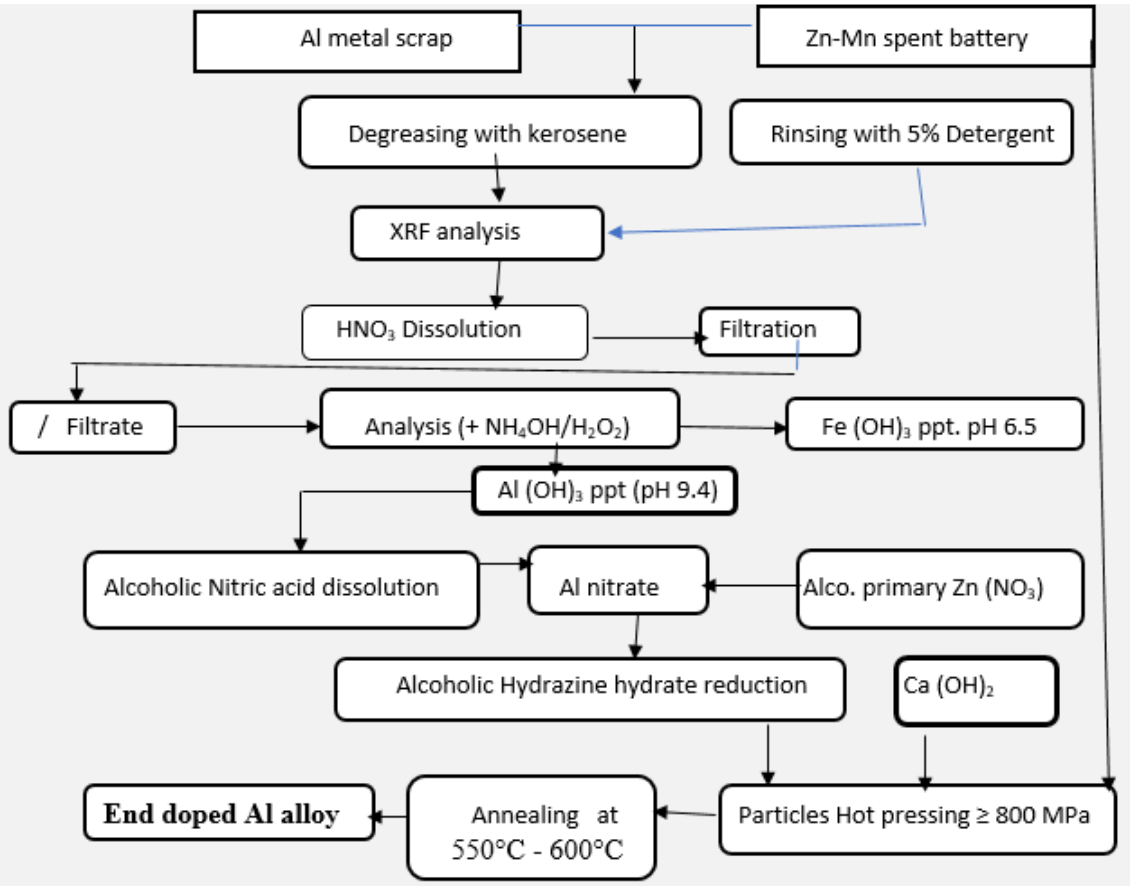

Figure 4: Sequential processing diagram for preparation of valuable 6061 alloys from Al metal scrap.

The composition of the aimed Al alloy is given in table 4

Table 4: The aimed composition of the prepared Al alloy.

Element	Wt. pct
Aluminium, Al	≈ 83
Copper, Cu	≤0.05
Magnesium, Mg	≤ 0.16
Manganese, Mn	<0.50
Nickel, Ni	<0.35 0.0-1.0
lime	<0 – 20 < 0.50
Zinc	
Other	

Methods of measurement of the physic-mechanical properties

The metal hardness was measured using, Vickers hardness tester series EVO by QATM combines extremely short cycle times with maximum precision.

The apparent density was measured by the pycnometer water displacement technique.

Identification and determination of metal content worked out by X-ray fluorescence spectroscopy (XRF) and XRD measurements.

The atomic spacing of crystalline structure was determined by bypassing an electromagnetic wave of known frequency through the material, and applying Bragg law ($n\lambda = 2d \sin\theta$). When $n = 2$ there is only one wavelength along with path CB; also, the reflected angle will be smaller than that for, say, $n = 3$.

Scanning microstructure analysis manifested by scanning electron microscope. Tescan Inc, USA, XRF (X-ray fluorescence), LIBS laser-induced breakdown spectroscopy, PANGA: prompt gamma neutron, activation analysis, XRT: (X-ray transmission).

Bond length.

Although both bands are between the same pair of elements, they can have different bond lengths.[21].

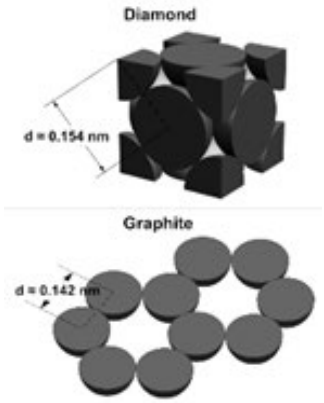

Results

Fig. 1 shows the graphical abstract containing the SEM micrograph of the Al alloy 6061. Fig. 2 shows a photograph of the metal's nonferrous (Fig. 2a) and mixed ferrous and nonferrous scrap (Fig. 2b). Fig. 3 shows a laboratory-scale fluidized bed jet mill (Fig. 3a) and the powdered scrap (Fig. 3b). Fig. 4 shows a sequential processing diagram for the preparation of valuable doped Al alloys from Al scrap. Fig.5 shows the effect of different solids (the scrap): liquid (HCl acid) ratio at 85 °C on the extent of leaching of metals in the scrap after removal of copper-It can be seen that the extent of leaching decreases in the order, Sn. Zn, Al, Fe, and nickel. Other metal of Si doesn't dissolve.

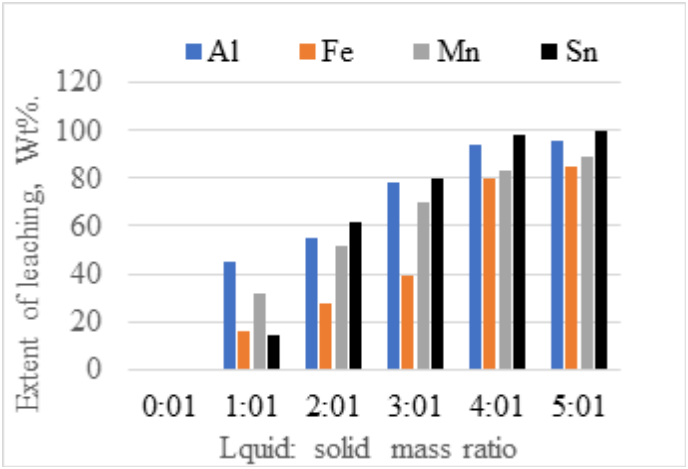

Figure 5: Effect of liquid: mass ratio on the extent of leaching.

Fig.6 shows the extent of dissolution of the metals in 3M HNO_3 at 75°C. It can be seen that magnesium readily dissolves in the nitric acid whereas other metals display a lower rate of dissolution which decreases in the order Fe, Al, Mn and Ni. Silicon is resistant to acid attack.

It can be seen that magnesium readily dissolves in the HCl acid whereas other metals display a lower extent of dissolution decreasing in the order Fe, Al, Mn and Ni. Silicon is resistant to acid attack.

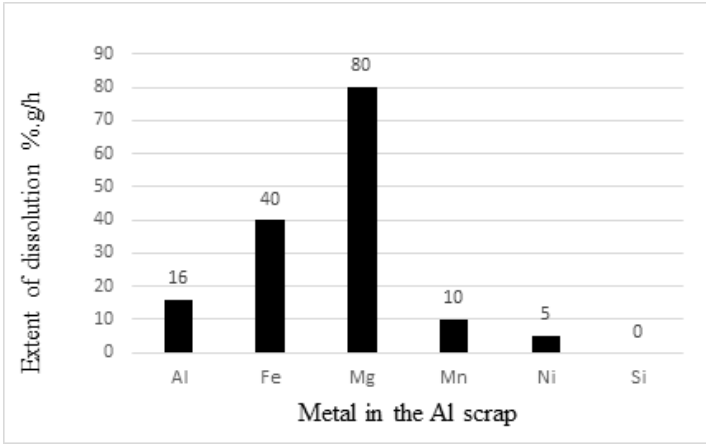

Figure 6: The extent of dissolution of some metals in the Al scrap in 3 M HNO_3 at 75°C.

Fig. 7 shows the effect of time on the weight pct of lime doped in the aluminium alloy at 900 °C by pyrometallurgy (PM) method. It is seen that the doped weight of lime is a time-dependent process whereby the maximum extent of the doped lime amounts to 0.62 pct and takes place after

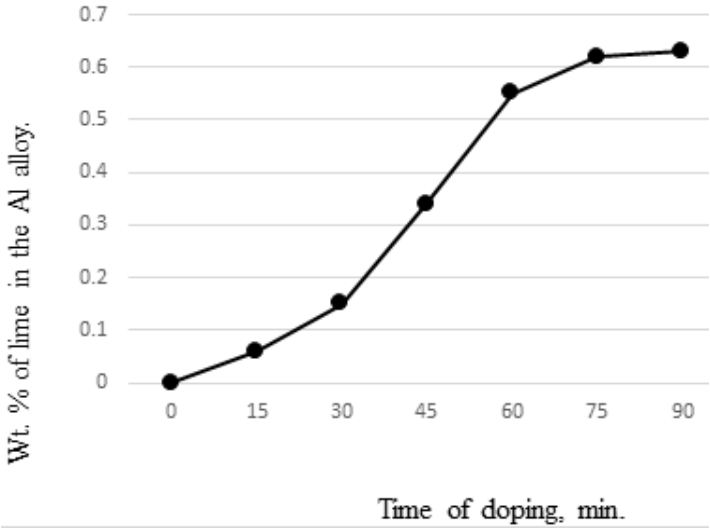

Figure 7: Effect of time of doping, min on Wt. % of lime in the Al alloy

90 minutes at 900 °C. Fig. 8 shows the weight of the doped lime in the Al alloy prepared by the powder metallurgy method (PM). It can be seen that the lime content that doped the Al alloy is much higher as compared to the pyrometallurgy method worth noting that the Al alloy turned less ductile.

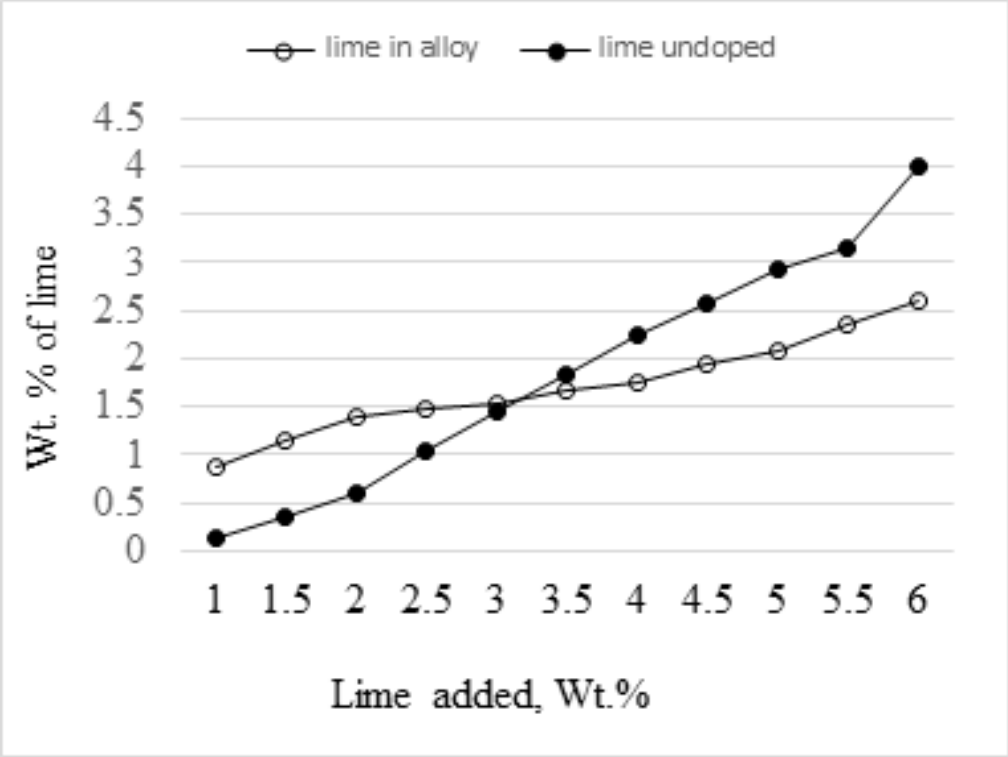

Figure 8: Lime doped in the Al alloy by PM method

Table 5 shows the weight pct of the doped lime and zinc of molten Al alloy as a function of time

Table 5: The weight pct of the doped lime and zinc of the molten Al all

Time of doping, min.	**Doping material**	**The added weight (g)/100 g Al**	**The doped weight**	**Pct of doped metal**
10	Lime	1	0.015	1.5
10	Zn	1	1.0	100
30	Lime	2	0.35	17.5
30	Zn	2	2	100
45	Lime	3	0.85	28.3
45	Zn	3	3	100
60	Lime	4	1.14	285
75	Lime	5	1.4	28.0
90	Lime	6	1.6	26.6

Fig.9 shows the effect of zinc addition on the hardness of the dopped Al alloy. It can be seen that zinc addition with ≥ 8 pct weight pronouncedly increases the hardness of the Al alloy. The ultimate hardness of the Al alloy is dopped with 20 % Wt. zinc amounts to 76 HRV.

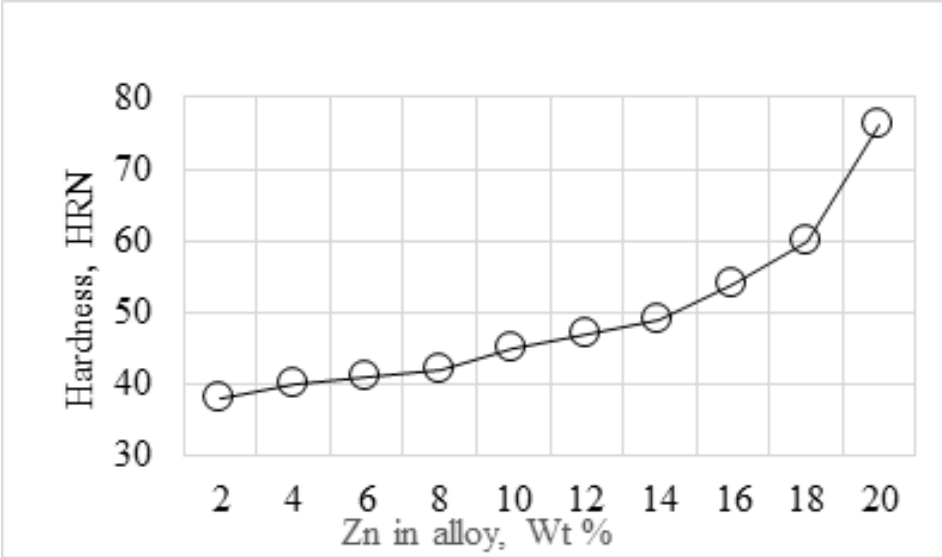

Figure 9: Effect of zinc addition on the hardness of the dopped Al alloy by PM.

Fig. 10 depicts the change in hardness upon the addition of Ca to the Al alloy. Calcium increases the hardness to less extent compared to zinc. With 10 Wt. % Ca the ultimate Al hardness amounts to 42 HRV.

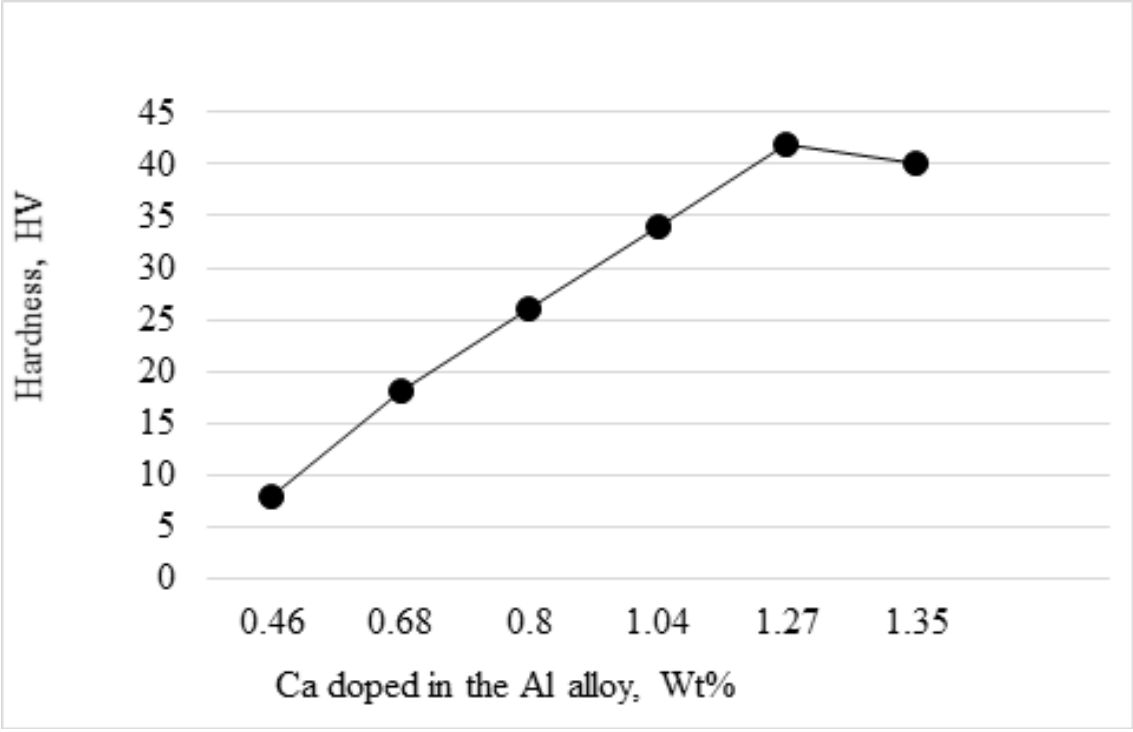

Figure 10: Effect of Ca doped in the Al alloy on the hardness of the Al alloy.

It is seen that calcium in the recovered alloy increases the mechanical hardness with the corresponding increase of calcium content to about 37 HV and 42 HV with 7 % and 10 % respectively. The mechanical hardness displays minor change with a further increase in calcium content of more than 10 Wt.%.

Fig. 11 shows the Arrhenius plot of the process of recovery of Al Alloy from scrap. 6061

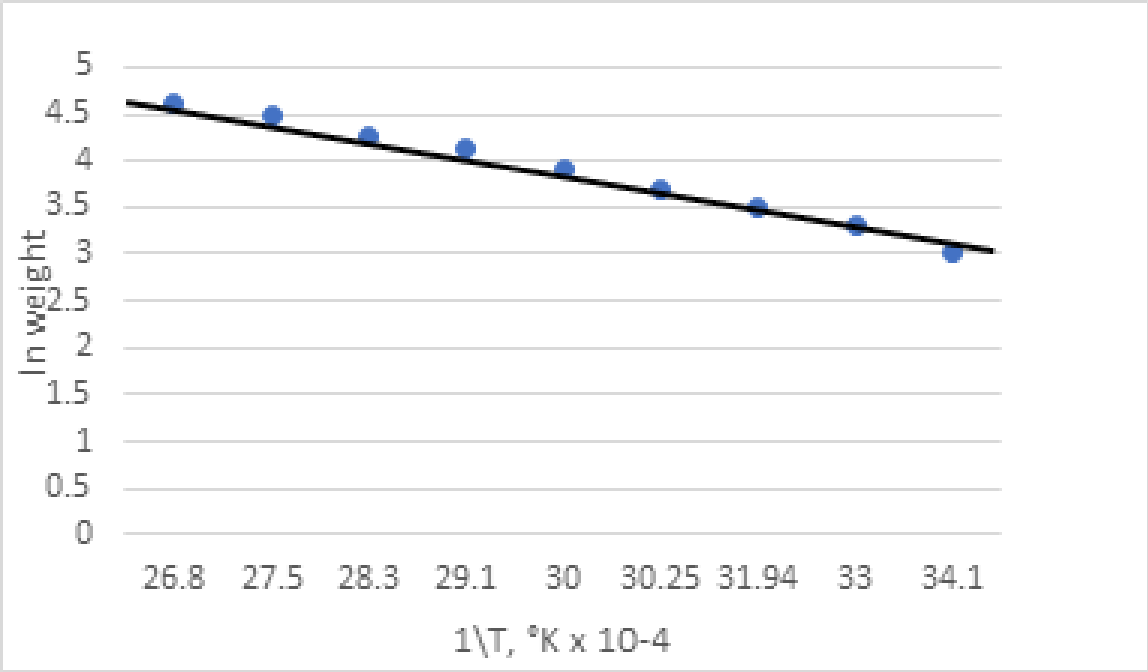

Figure 11: the Arrhenius plot of the process of recovery of Al Alloy from scrap. 6061

Fig. 12 a-b shows the effect of the addition of Zn and Ca to the Al alloy 6061 on its density (12a) and microstructure (Fig. 12b). It is seen that zinc addition increases the Al alloy whereas calcium addition decreases the alloy.

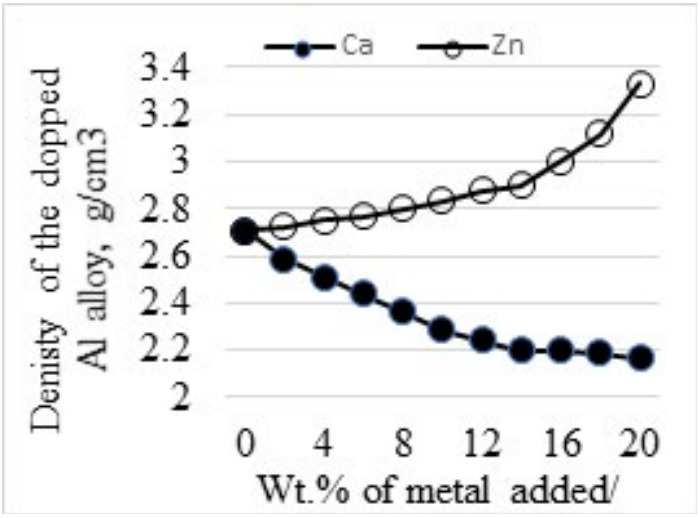

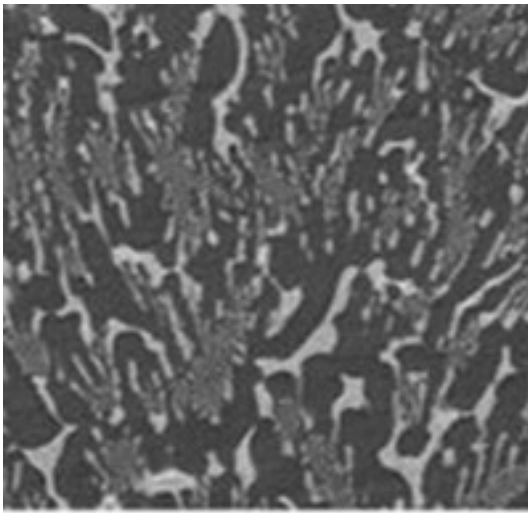

Figure. 12a The density of Al with up to 20 Wt. % Zn and Ca

Figure. 12b SEM of 1Al 1%Zn and 3%Ca

Figure 12: The effect of the addition of Zn and Ca to the Al alloy 6061 on its density (12a) and microstructure (Fig. 12b).

Fig. 13 shows the Gibbs free energy of the formation of different Al_xCa_y alloys within the temperature range of 620°C - 675 °C for fixed periods of 30 minutes. It is seen that the ΔG energy for Ca addition to Al metal slightly decreases linearly with temperature up to 675 °C.

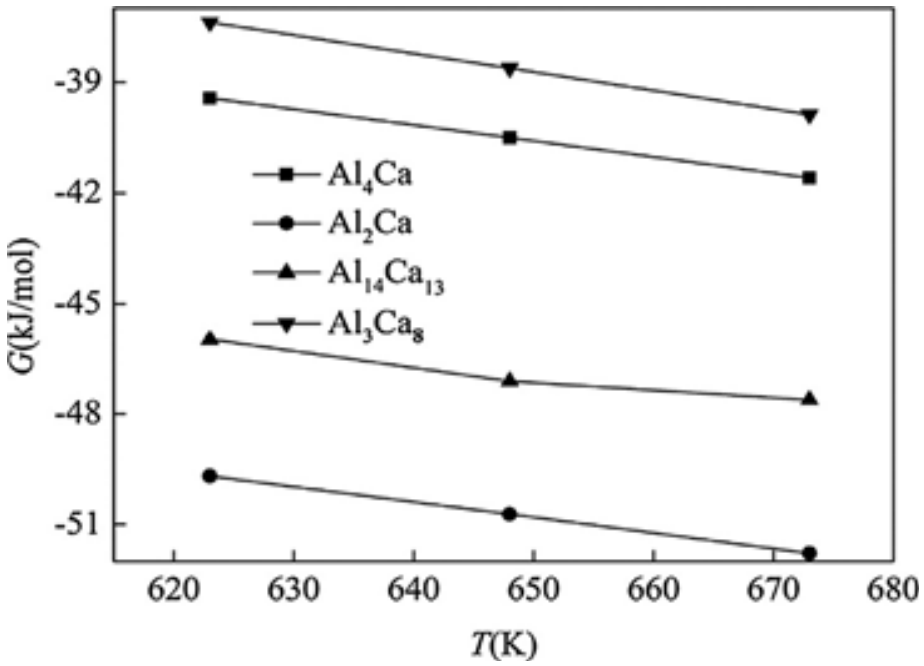

Figure 13: The Gibbs free energy of the formation of different AlxCay alloys

The activation energy of the process of Ca addition was calculated from the Arrhenius plot given in Fig 14 and found to be 27.533KJ. mol^{-1}.

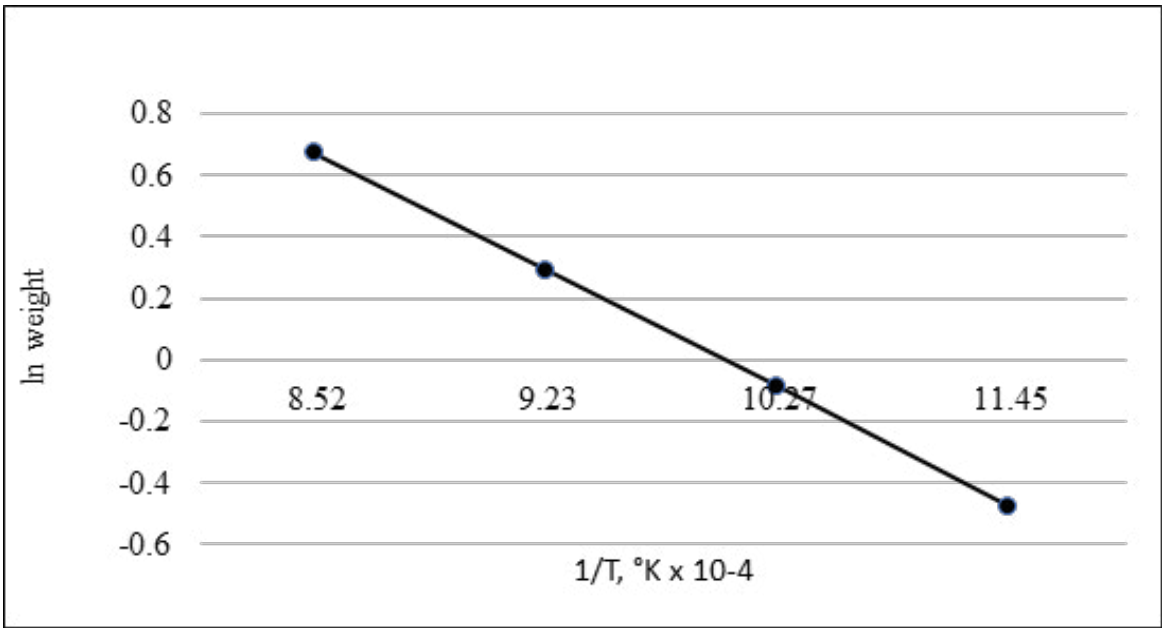

Figure 14: The activation energy of the process of Ca addition on Al alloy.

Fig. 15 shows the X-ray diffraction pattern of the Al3Ca2La1.5Mn alloy given in comparison with the binary Al14Ca alloy. Zhuliang 2022

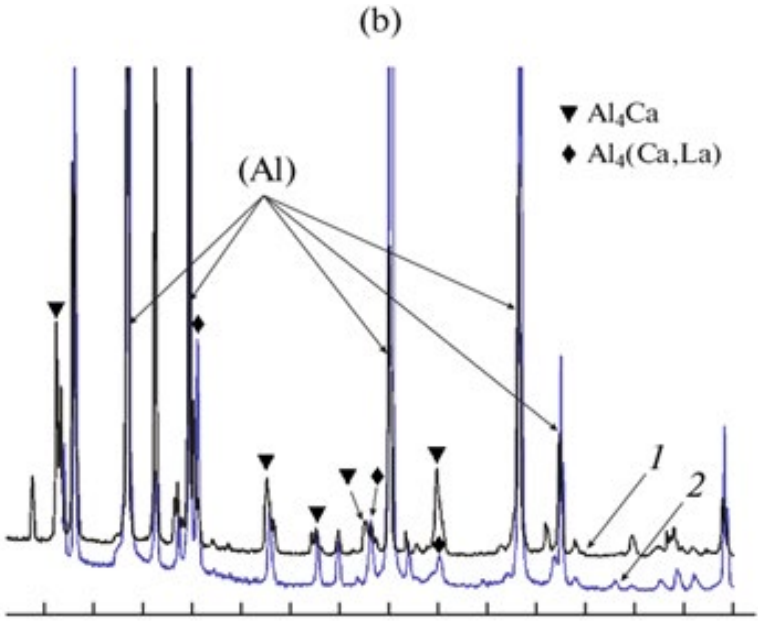

Figure 15: The X-ray diffraction pattern of the Al3Ca2La1.5Mn alloy given in comparison with the binary Al14Ca alloy, Zhuliang 2022.

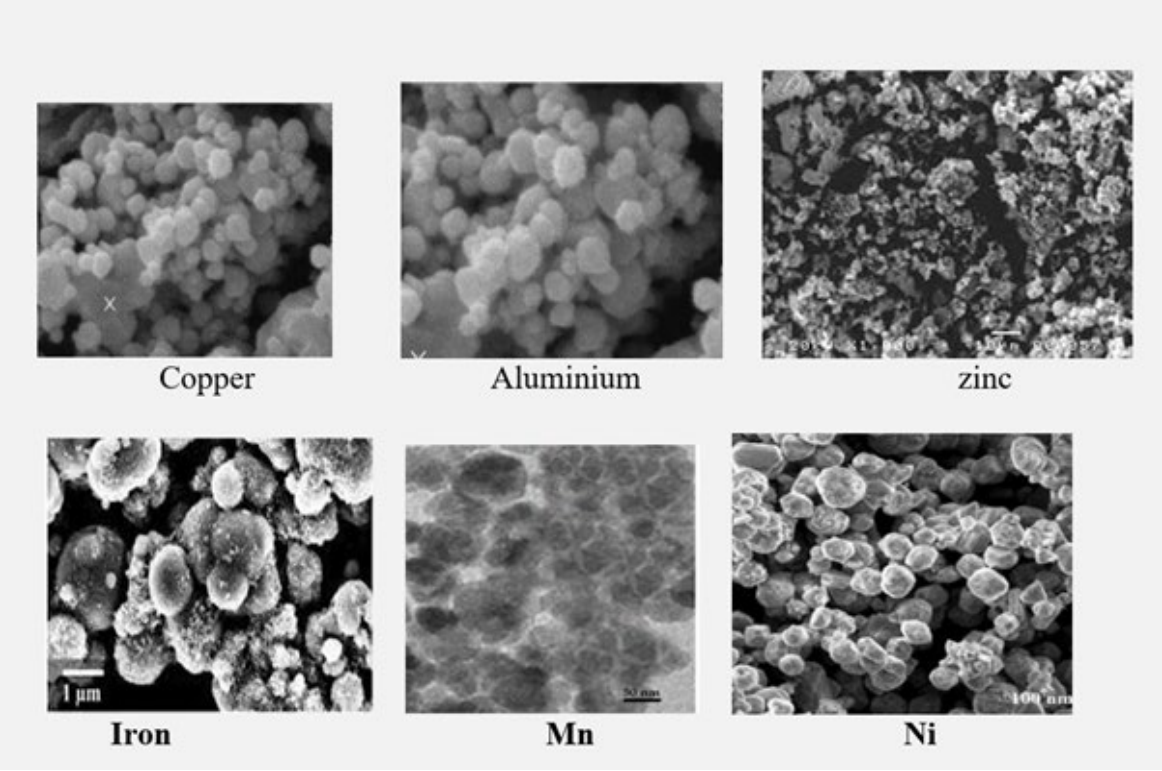

Figure 16: SEM images of some metals obtained by reduction of their salts with 1 M ascorbic acid solution.

It can be seen that the alloying metals ≥ 0.5 Wt.% appeared in the scanned image. Fig. 17a.b, shows the SEM of the annealed aluminium alloy containing 4 % calcium at 550 °C for 10h. after annealing for10 h

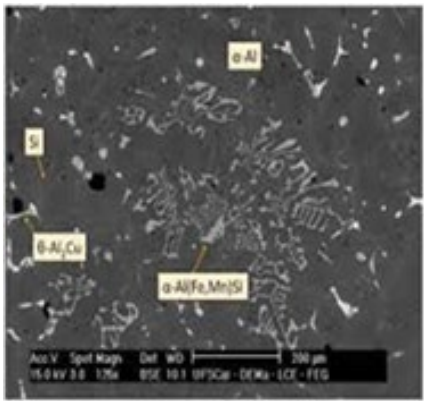

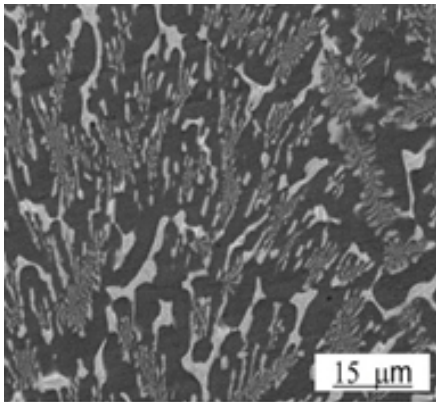

Fig. 17a **Fig. 17 (b)**

Figure 17 :a.b: SEM image of the recovered alloy (a) and with 1.2 % Ca microstructure,

It is worthy to note that the effect of the addition of other metals on the physical properties of the recovered Al 6061alloy deviates the produced alloy from the specifications assigned for 6061 alloy and forms alternative alloys with unspecified standard composition. Therefore, only the standard Al 6061 alloy as specified was strictly followed in this study. In the next phase, such an effect will be studied. The advantage of the present method in comparison with the other methods of recycling is that it can be carried out with lower energy consumption, simple and the output efficiency amounts to 98.7 %.

Lime inclusions improved the physical and mechanical properties of the prepared alloy, although it increases the hardness of the alloy by approximately 37 V. Calcium is widely used for reduction purposes but may limit its extensive industrial use in lightweight structures. The activation energy of the alloy preparation method amounts to 27.53 kJ/mol with a recovery potency of 98.7%.

Discussion

Calcium particles may display as grain refiners for primary base alloy. Such role helps in improving the strength of the virgin alloy. Calcium atomic radius. Other metals in the scrap undissolved in the alkaline reagent containing hydrogen peroxide, and. after filtration, revealed that copper went into the solution. The solid residue leached by 3 M HCl solution to produce soluble chloride salts as follows

$$xM + yHCl \longrightarrow MxCly + yH_2 \ldots \quad (7)$$

The metals chloride in the solution was analyzed with the help of ICP and the required mole was adjusted either by partial precipitation of the metal in excess to form an insoluble compound or by the addition of a freshly prepared solution from a primary salt of the metal of concern. The calculated volume of the metal's chloride solution was then mixed with copper test ammonia and magnesium silicide and thoroughly stirred. Metal ions in the global solution were reduced chemically with hydrazine hydrate of ascorbic acid as follows. Ascorbic acid has the following structure whereby the (….H) is the active reducing atom

The reaction with MCl_2 to give free metal particles takes place according to

Metal chloride + ascorbic acid ⟶ free metal particles + oxidized ascorbic acid + HCl acid

$$2MCl_2 + 3C_6H_8O \longrightarrow 2\,M + 3C_6H_6O + 4\,HCl \ \ldots\ldots\ldots .(6)$$

Similarly, hydrazine hydrate reduces the metal ions according to

$$NH_2NH_2.H_2O + 2MCl_2 \longrightarrow M + N_2H_2 + 4\,HCl \ldots\ldots\ldots\ldots(7)$$

nickel nanoparticles were obtained by chemical reduction of their respective salt solution using 1M ascorbic acid at room temperature. Magnesium and silicon content were managed by the addition of the freshly prepared magnesium silicide. Fig 3 shows the structure of Mg silicide. Silicon occupies the centres and the corners of the face-cantered cubic lattice. and Mg centres occupy eight tetrahedral sites in the interior of the unit cell. Fig. 2 shows a photograph of the metal scrap.

The Al alloy No. 6061 is highly recommended in structural applications where lightweight or corrosion resistance is required. The alloy, composed mostly of aluminum, displays importance in aerospace manufacturing. The alloy is used for the production of electronic and microelectronic components and radar construction. Microstructural characterization is 231nm and 125 nm (Van der Vaal and empirical values respectively) as compared to aluminum (184nm) or zinc (139nm). The addition of calcium to the Al alloy involves partially displacement of the host Al atoms causing a decrease in the density of the host alloy as revealed in Fig. 18a. the changes in the structure of the alloy may be postulated as represented in Fig. 18a

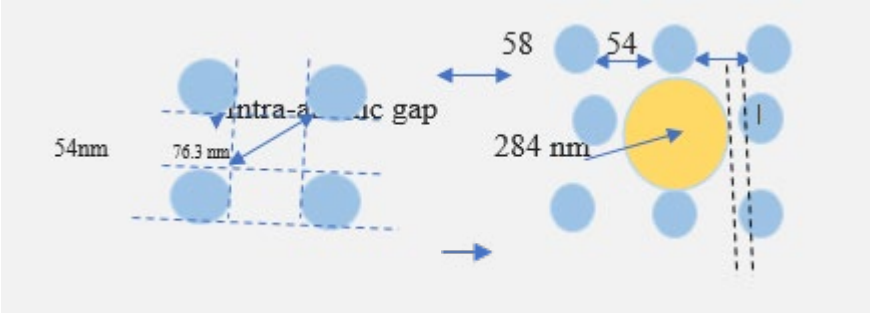

Typical atomic structure of Al the atomic structure of Al

Figure 18a: Partial displacement of the host Al atoms causing a decrease in the density

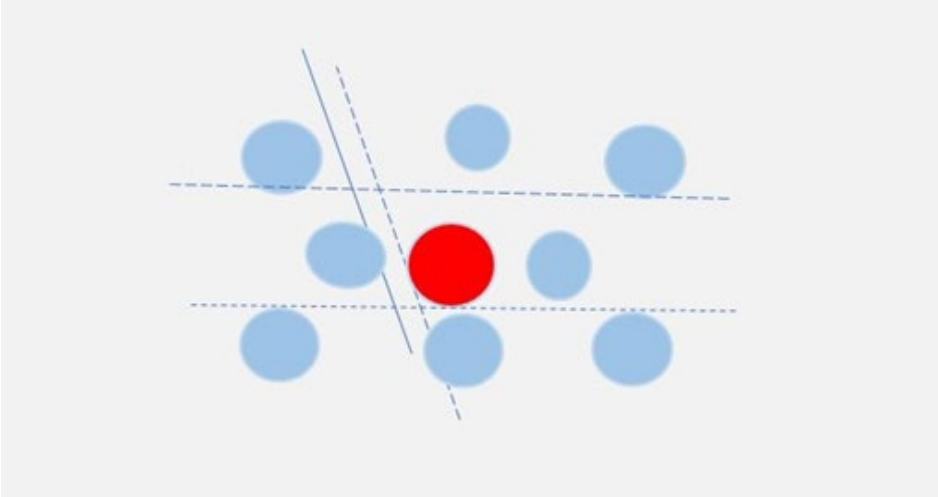

Figure18b: Possible atomic structure of the Al 6061 alloy after the addition of Ca

The hypothetical density value of the Al alloy Al4Ca amounts to 2.95 g.cm^{-3} Because the alloy microstructure is not perfectly ideal but with intra-atomic space. it would be legitimate to expect a decrease in density of the Al (ρ = 2.71) 6061 alloy upon the addition of calcium (ρ =1.55). The extent of decrease relates to the Ca weight doped in the host alloy until Ca satisfies the available spaces. Zinc on the other hand has a smaller atomic radius and higher density value as compared to calcium. Therefore, the addition of zinc causes an increase in density value as shown in fig. 11a. The results shown in Fig. 10a are in line with the postulated model as demonstrated above. However, because the density value of zinc metal is higher than with calcium and the atomic radius is smaller, it would be expected that the addition of zinc opposes that of calcium i. e the density increases The Gibbs energies of formation of Alcan alloys confirm that higher energy values would be consumed as the Ca mass ratio goes up. The traditional name of Al 6061 with calcium is produced under the name Alcoa. Alcoa wheels are forged from one single block of high strength aluminum alloy. This alloy is 5 times stronger than steel wheels and withstands the most severe tests, LBF, TUV, and JWL-T. Alcoa workhorse wheels have no ventilation holes, to protect the disc brakes in off-road applications. The addition of the alloying metals involves heating on-site to the required temperature and stirring. The extent of the activation energy of the Al-Ca/Zn alloys preparation method amounts to 27.53, kJ/mol with a recovery potency of 98.4 % obtained from the plots of the extent of recovery versus absolute temperature (figs. Not presented).

Fig. 19 shows The XRD pattern of the different Al-alloys containing Zn, Ca and other metals. It is seen that with aluminum metal, the peaks appearing at 2Θ of 42, 45, 67 and 78 displayed the highest intensity value of ≥2000. With aluminium alloys, the 2Θ peaks appeared at the same 2Θ value but with lower intensity of 500 up to 1800. The peak's intensity relates to the alloying element in the order Zn, Cu and Mg.

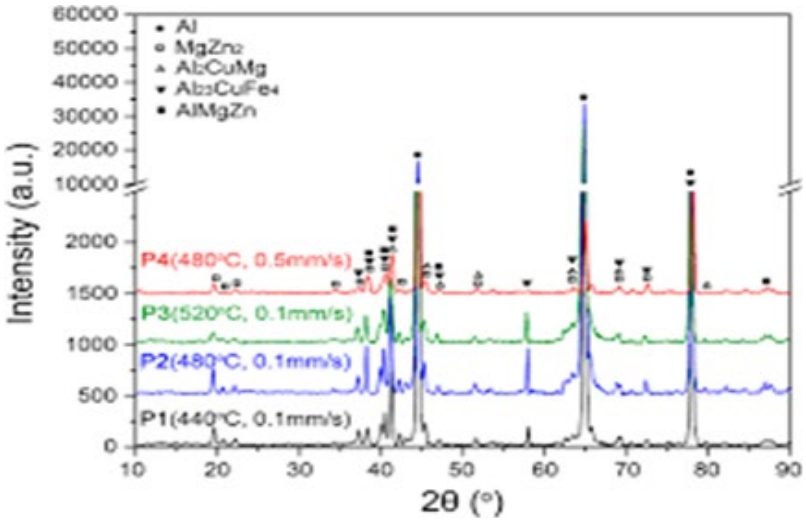

Figure 19: XRD pattern of the different Al-alloys containing Zn, Ca and other metals

Conclusions

The output conclusion of this study can be summarized in the following. The metal Al scrap is a recurring source of metal values like copper, aluminum and nickel. There is no guarantee, during the primary machining, for assorting the scrap from being mixed and may be wasted as a scrap. The weight percentage of the metals is variable and differs from one workshop to another depending on the countryside and type of the industry. Direct melting of the scrap doesn't score the goal recovery of 6061 alloys because of the broad variety of the melting point of the elements available. The suggested method involves magnetic separation of the ferromagnetic elements, hydrometallurgy selectively leaching of copper in alkaline ammonium hydroxide/ammonium bicarbonate solution containing 10 % H_2O_2, filtration of the reaction medium and leaching of the remaining unreacted metals with 3M HCl at room temperature becomes the suitable way to achieve preparation of the targeted Al 6061 alloy. Calcium addition to the alloy improves the alloy's hardness. Calcium is a reducing agent for many reactive, less common metals; to remove impurities from lead; as a desulfurizer and deoxidizer for ferrous metals and alloys; and as an alloying agent for aluminum, silicon, and lead. Calcium is widely used for this purpose. The precise and accurate composition of the 6061 alloys is easily workable. Controlling the portion of the metals solutions that are then mixed and reduced with 1 M ascorbic acid produces metal powders constituting the 6061 alloy composition.

References

1. Amini Mashhadi, H., Moloodi, A., Golestanipour, M., & Karimi, E. Z. V. (2009). Recycling of aluminium alloy turning scrap via cold pressing and melting with salt flux. Journal of materials processing technology, 209(7), 3138-3142.
2. Bhuyan, A. (2021). Circular Economy Scenario in India. Adn Envi Was Mana Rec, 4 (3): 223-225.
3. Stock, A., & Somieski, C. (1916). Siliciumwasserstoffe. I. Die aus Magnesiumsilicid und Säuren entstehenden Siliciumwasserstoffe. Berichte der deutschen chemischen Gesellschaft, 49(1), 111-157.
4. Handbook, M. (1990). Properties and Selection: Nonferrous Alloys and Special-Purpose Materials, 10th.
5. Edtmaier, C., Schiesser, R., Meissl, C., Schubert, W. D., Bock, A., Schön, A., & Zeiler, B. (2005). Selective removal of the cobalt binder in WC/Co based hardmetal scraps by acetic acid leaching. Hydrometallurgy, 76(1-2), 63-71.
6. Harandi, S. E., Mirshahi, M., Koleini, S., Idris, M. H., Jafari, H., & Kadir, M. R. A. (2013). Effect of calcium content on the microstructure, hardness and in-vitro corrosion behavior of biodegradable Mg-Ca binary alloy. Materials Research, 16, 11-18.
7. nwood, N. N and Alan E. Chemistry of the Elements (2nd ed.). Butterworth- H.J. Axon, D., Phil and W., Hume-Rothery, F.R.S, "The lattice spacings of solid solutions of different elements in aluminum" The inorganic chemistry laboratory. Laboratory, University of Oxtford, 1997. 1-24, Downloaded from https://royalsocietypublishing.org/ on 16 April 2022 Heinemann. ISBN 978-0-08-037941-8.
8. https://www2.yamaha-motor.co.jp Yamaha Japanese Industrial Standards Data. 2021
9. Muchova, L., Eder, P., & Villanueva, A. (2011). End-of-waste criteria for copper and copper alloy scrap: technical proposals. JRC Scientific and Technical Report, Scientific and Technical Research series, 18.
10. Joost, R., Pirso, J., & Viljus, M. (2008). Recycling of Hardmetal Scrap to WC-Co Powder by Oxidation-Reduction Process. na.
11. Hisayoshi, K., Uyeda, C., & Terada, K. (2016). Magnetic separation of general solid particles realised by a permanent magnet. Scientific Reports, 6(1), 1-6.
12. Chen, L., Li, Y., Tang, J., Zhao, G., & Zhang, C. (2019). Investigation on microstructure and mechanical properties of Al–5.50 Zn–2.35 Mg–1.36 Cu alloy fabricated by hot extrusion process. Journal of Materials Research, 34(18), 3151-

3162.
13. Sulzakimin M, Siti Fatimah O and Sulzarina M (2021) Issues on a Solid Waste Management System in Cameron Highlands, Malaysia. Adn Envi Was Mana Rec, 4(3):229-231.
14. Mat Web material property data, 6061 Aluminium composition data. Internet 2021.
15. Hirayama, N., Iida, T., Sakamoto, M., Nishio, K., & Hamada, N. (2019). Substitutional and interstitial impurity p-type doping of thermoelectric Mg2Si: a theoretical study. Science and technology of advanced materials, 20(1), 160-172.
16. Laverty, P. D., Atkinson, G. B., & Desmond, D. P. (1989). Separation and recovery of metals from zinc-treated superalloy scrap (Vol. 9235). US Department of the Interior, Bureau of Mines.
17. Feher, F. (1963). Handbook of preparative inorganic chemistry. Vol. I, G. Brauer, Ed., Academic Press, NY, 418.
18. P. G. Barnard, and H. Kenworthy US Patent 3,595,484., 1969.
19. Katiyar, P. K., Randhawa, N. S., Hait, J., Jana, R. K., Singh, K. K., & Mankhand, T. R. (2014). An overview on different processes for recovery of valuable metals from tungsten carbide scrap.
20. r, Leblanc, "An Introduction to Metal Recycling" Updated March 05 1971, 202
21. Dièye, S., & Faye, C. Ababacar Fall and Pierre Corneille Sambou (2021) Use of the standardized precipitation and evapotranspiration index (SPEI) from 1961 to 2019 to characterize the drought trend in northern Senegal: Study of the spatio-temporal dynamics in the Ferlo watershed. Adn Envi Was Mana Rec, 4 (3): 232-244.
22. Kumari, S. S., Pillai, R. M., & Pai, B. C. (2005). Role of calcium in aluminium based alloys and composites. International materials reviews, 50(4), 216-238.
23. WH, S., & Chun T.. Wang. (1979). Tungsten: sources, metallurgy, properties, and applications. Plenum press.
24. Akopyan, T. K., Letyagin, N. V., Sviridova, T. Y. A., Korotkova, N. O., & Prosviryakov, A. S. (2020). New casting alloys based on the Al+ Al4 (Ca, La) eutectic. JOM, 72(11), 3779-3786.
25. Borisenko, V. E. (2013). Semiconducting Silicides: Basics, Formation, Properties (Vol. 39). Springer Science & Business Media.
26. Hunt, G., Peters, A., Spicer, J., & Thomas, M. High Temperature Optical Performance of Mgo: Y 2 O 3 Films for Space Applications. Available at SSRN 4045893.
27. Wikipedia, (2021). "Structure of Mg silicide,the free Encyclopedia, Internet online.
28. Wikipedia, (2022). the free encyclopedia Bond length, Internet.
29. Wikipedia. (2022). org the free encyclopedia, Online Internet 2022Atomic radii of the elements.
30. www. machine design. "World's strongest aluminum alloy" APR 26, 2007
31. Noda, Y., Kon, H., Furukawa, Y., Otsuka, N., Nishida, I. A., & Masumoto, K. (1992). Preparation and thermoelectric properties of Mg2Si1− xGex (x= 0.0□ 0.4) solid solution semiconductors. Materials Transactions, JIM, 33(9), 845-850.
32. Li, Z., Ding, H., Huang, Y., & Langdon, T. G. (2022). An Evaluation of the Mechanical Properties, Microstructures, and Strengthening Mechanisms of Pure Mg Processed by High-Pressure Torsion at Different Temperatures. Advanced Engineering Materials, 24(10), 2200799.